MAPPING THE DROPLET DRYING PHENOMENA WITHIN A FLUIDIZED BED COATER AS A PREDICTION TOOL FOR COATING QUALITIES

Fesia L. Laksmana, University of Groningen, Groningen, The Netherlands
Paul J.A. Hartman Kok, Schering-Plough, Oss, The Netherlands
Herman Vromans, Schering-Plough, Oss, The Netherlands
Henderik W. J. Frijlink, University of Groningen, Groningen, The Netherlands
Kees Van der Voort Maarschalk, Schering-Plough, Oss, The Netherlands
Abstract ID: 126005

Introduction

For a high coating quality, agglomeration and excessive evaporation of the coating droplets during fluidized bed coating process should be avoided (1-3). This means that the coating process can often only be performed within a narrow operating window. Consequently, the selection of the process conditions and the process control are delicate steps to assure a good coating quality.

In spite of being an established technology, the process development of a fluidized bed coating process has often been performed in an empirical way. This approach obviously results in a large experimental program and the interpretation of the results stays far from first principles. In this manner, a rapid and continuous process development is difficult to be achieved. Process modeling is one of the methods that can aid the process understanding, as it enables a comprehensive parametric study of the involving sub-processes and further can be used as a process prediction tool once it is validated.

In this study, the physical phenomena occurring during a single droplet drying within a fluidized bed coater have been modeled, comprising of the changes in the droplet mass, water fraction, droplet size and droplet shape in time, before and after collision with the core particles. Using the models, the influence of various process conditions, i.e. inlet air temperatures, atomization pressures, and spraying rates could be studied comprehensively. The coatings obtained from the corresponding processes were characterized using a previously developed quantitative image analysis method (4, 5). In this way, the relationship between the extent of the droplet drying and the obtained coating quality could be assessed, which makes the model also usable as a development tool.

Heat and Mass Transfer Models

Inside a fluidized bed coater, the journey of droplets starts from being atomized from a spraying nozzle, colliding with core particles, spreading and further being dried and leaving deposit on the core surface as coating layer (3) (Figure 1). The drying conditions (temperature and vapor pressure) of the droplets were calculated using a mass and heat balance, where the total volume of the equipment was taken as the control volume and steady state mass and energy transfers were assumed. The mass and heat transfer between a single droplet and the hot-humid air can be expressed as Eq. 1. The heat transfer coefficient h was calculated using the established correlations (6). Different considerations were given during the modeling, according to the different stages that a droplet undergoes before it is completely dried.

During droplet's traveling period, the drying process of a droplet could be modeled quite straight-forwardly, assuming a spherical droplet wherein only changes in the water retained in the

droplet and droplet diameter occur in time. Once the droplet hits the core particle, the droplet spontaneously spreads on the core surface, which extent depends on the impact (inertia spreading) and the surface energy (wet spreading) (7). Consequently, the changes in the droplet forms from spherical to spherical cap were taken into account in the drying model. Due to evaporation, the droplet contact line is receding (8). This occurs by keeping the contact angle more or less constant. Once the solute concentration increases to a critical value, pinning occurs. During pinning, the droplet diameter stays constant, while the droplet height decreases significantly (9). The transition between these two evaporation regimes is to be determined in this study, which influences the droplet deposit type i.e. dot-like or ring-like and therefore the coating quality. Eqs. 2-4 depict the drying models used to simulate the changes in the droplet mass in time at different periods, during i.e. droplet traveling, receding contact line period, and pinning period, respectively. In these models, shrinking control volume was assumed and linear correlation between the water fraction remained and the solution physical properties. These models were derived by substituting a set of correlations between droplet properties and its mass into Eq. 1.

$$\frac{dm}{dt} = -\frac{dQ/dt}{\lambda} = -\frac{hA(T_{a,in} - T_{wb})}{\lambda} \tag{1}$$

$$\frac{dm}{dt} = -\frac{(T_{a,in} - T_{wb})}{\lambda} \pi k(m) \left\{ 2 \frac{6}{\rho\pi}^{1/3} m^{1/3} + 0.65 \frac{\rho_a u_a}{\mu_a}^{0.5} \frac{\mu_a Cp_a}{k_a}^{1/3} \frac{6}{\rho\pi}^{0.5} m^{0.5} \right\} \tag{2}$$

$$\frac{dm}{dt} = -\frac{(T_{a,in} - T_{wb})}{4\lambda} \pi k(m) \left(1 + tan^2\left(\frac{\theta}{2}\right)\right) \cdot$$

$$\left\{ 4 \left(\frac{6}{\rho\pi\left(3tan\left(\frac{\theta}{2}\right) + tan^3\left(\frac{\theta}{2}\right)\right)} \right)^{1/3} m^{1/3} + 1.84 \left(\frac{\rho_a u_a}{\mu_a}\right)^{0.5} \left(\frac{\mu_a Cp_a}{k_a}\right)^{1/3} \left(\frac{6}{\rho\pi\left(3tan\left(\frac{\theta}{2}\right) + tan^3\left(\frac{\theta}{2}\right)\right)} \right)^{0.5} m^{0.5} \right\} \tag{3}$$

$$\frac{dm}{dt} = -\frac{(T_{a,in} - T_{wb})}{4\lambda} \pi k(m) \left\{ 2d_{col} + 0.65 \frac{\rho_a u_a}{\mu_a}^{0.5} \frac{\mu_a Cp_a}{k_a}^{1/3} d_{col}^{1.5} \right\} \cdot$$

$$\left(1 + \left(\frac{6}{\rho\pi\left(3tan\left(\frac{\theta}{2}\right) + tan^3\left(\frac{\theta}{2}\right)\right)} \right)^{-2/3} m^{-2/3} h(m) \right) \tag{4}$$

The critical conditions used for the simulation at which the transition between the receding contact line and pinning regimes occurs were determined using the thermal gravimetric analysis (TGA) data. For each evaporation regime, a model was used, where the transition between the two regimes was optimized based on the goodness of the fit of the data to both of the models.

Material and Methods

Materials

Microcrystalline cellulose/MCC (Avicel PH102, FMC BioPolymer) was used as pellet excipient. Hydroxy-propyl methylcellulose/HPMC (Methocel E5 LV USP/ EP premium grade, Dow) was used as coating model material. Carmoisine (E122, Pomona BV) was used as pigment in the coating.

Experimental Methods

1.   Pellets Production

The pellets were made in a high shear granulator (GRAL 10, Machines Colette, Belgium), with impeller and chopper rates of 600 and 3000 rpm, respectively. The pellets were made by mixing 500g of MCC with 500g of water, which was poured slowly (in 1 minute time) from the top of the GRAL. The granulation was performed for 20 minutes. The wet granules were further dried at 40°C for 8 hours in the vacuum drier (Elbanton, The Netherlands).

2.   Particle Coating

The pellets with size fraction of 800-1000 micron were coated in the fluidized bed coater (Mycrolab, Hüttlin, Germany). 150 g of pellets was used for each batch. The coating solution can be fed either from the bottom or the top of the column. Furthermore, the spray rate, drying temperature, and atomization pressure were varied. The coating process was performed until 20% weight ratio of coating to core was sprayed. The sprayed HPMC solution was HPMC (5% w/w water) and carmoisine (0.1% w/w water) dissolved in cold water.

3.   CSLM and Image Analysis

The carmoisine added to the coating fluoresces enabling the visualization of the coating layer under the CSLM and differentiate the coating layer from the core. A Leica inverted microscope DM IRE2 TCS SP2 (Leica microsystems, Germany) was used to acquire images of coated particles. Immersion oil type B (Cargille Lab, USA) was added to the coated particles prior to scanning. A green laser (HeNe 543nm/1.2mW) and a red laser (HeNe 633nm/10mW) were set at 100% and 37.66% intensity. The emission of the sample was collected at 652-716 nm. An HC Plan Fluotar 10x/0.30 objective was used with a zoom factor of 1 or 10 resulting in scanned area of 1500µm x 1500µm or 150µm x 150µm, used to acquire images for the characterization of coating thickness and pore structure, respectively. Image analysis was performed on the acquired images, developed previously, allowing the measurement of the coating thickness distribution around a pellet, coating porosity and the pore size distribution (4, 5).

4.   Thermal Gravimetric Analysis (TGA)

The evaporation of a droplet of HPMC E5 solution (5% concentration) was followed using a TGA equipment (Mettler Toledo TGA/SDTA851^e, The Netherlands) at various the drying temperatures ranging from 40 to 80°C. For each temperature, the measurement was performed in three-fold. The droplet was dosed using Gilson micropipettes giving a 5 µl volume droplet and it was carefully dropped into a TGA aluminum 40 µl crucible. Continuous dry nitrogen gas flow at 40ml/min was

purged above the droplet solution inside the TGA. Performing the droplet evaporation in TGA also simulates a single droplet drying inside a fluidized bed coater to some extent. The obtained polymer films were visually observed to confirm the droplet pinning theory used in this study. Furthermore, the data was used to derive the critical conditions at which pinning occurs as a function of drying temperature.

Results and Discussion

Figure 2 (top) shows the effect of drying temperature on the obtained coating porosity. Here, only the results on coating porosity are presented, as comparable results were obtained on the coating thickness and pore size. It is shown that the coating porosity decreases with the decrease of inlet air (drying) temperature used. Using current models, the effect of process conditions, in this case the drying temperature, on the evolution of the droplet properties during drying were able to be simulated. Important characteristics, such as droplet diameter, height, contact angle, water fraction retained, droplet spreading flux and pinning time could be determined, which are relevant to the film formation and therefore coating quality.

Figure 3 and Figure 4 show the typical evolution of the droplet diameter and contact angle during drying inside a fluidized bed coater. It can be seen that initially the droplet size decreases during the droplet traveling and then increases several-fold due to the droplet-particle impact and afterwards decreases again due to further drying. The higher the drying temperature used during coating process, the smaller is the diameter of droplet when it hits the core particle. Furthermore, the contact angle of the droplet upon collision with particle is higher at higher drying temperature, which is actually due to the impact of the droplet size on the contact angle. It was also found that at higher drying temperature, the pinning occurs earlier. As the wetting diameter is higher, the average polymer concentration is lower, leading to a ring-like polymer deposit, and therefore a poor film. On the other hand, if the pinning is delayed, the droplet will more likely form a dot-like film (9). The findings from our TGA experiments confirm the plausibility of this theory. Furthermore, a lower contact angle also results in a better spreading of the droplet on the core surface. Considering the effect of drying temperature on the characteristics of the droplet drying and the coating structures, it can be implied that the changes in the coating porosity is actually due to the variation in the pinning time and the droplet contact angle.

Increasing the atomization pressure reduces the initial droplet size, of which the pinning time is slightly lower and the contact angle is increased. Additionally, lowering the droplet size increases significantly the droplet spreading flux of the droplet on the particle, which was calculated as the ratio between a droplet area on the core surface upon collision multiplied by the number of droplets sprayed and divided by the total area of the core particles. In this case, the effect of the increase in the droplet spreading flux is much more significant on the porosity, considering also that the reduction in the pinning time due to the decrease in the droplet size is very little. As a result, the coating porosity becomes lower for coating process using high atomization pressure.

Using a high spraying rate during the coating process increases the bed relative humidity and the droplet size at the same time. This causes a more complex effect of the spraying rate on the characteristics of the droplet drying and therefore the coating quality. While delaying the pinning time, the increase in the spraying rate also reduces the droplet spreading flux, which effects on the coating quality are counteracting with each other. Consequently, altering the spraying rate does not vary greatly the coating porosity.

Figure 5 summarizes the effect of the droplet spreading flux and the droplet pinning time on the coating porosity. It is shown that the coating porosity is the highest when the droplet spreading flux and the pinning time are low. At low droplet spreading flux (due to high spraying rate/low atomization pressure), a very high pinning time is required to reduce the coating porosity. This can be achieved by using the lowest drying temperature possible. In this region, the droplet type-deposition significantly influences the obtained coating structure. At high droplet spreading flux, the influence of the pinning time becomes less significant on the coating porosity. The resulted coating structures in this regime are very much governed by the dispersion of the droplets through the bed of the core particles. Using the presented simulations, it is possible to find the suitable set of process conditions to assure a low coating porosity, i.e. a good coating quality.

Conclusions

From current droplet drying modeling results, the importance of the droplet spreading flux and the droplet pinning time on coating quality has been identified. A delayed pinning time leads to a dot-like polymer deposition resulting in a better coating film. A high droplet spreading flux allows a high distribution of droplets on core surfaces, giving also a coating with low porosity. In combination, it is shown that at low droplet spreading flux, the pinning phenomena of a droplet during drying becomes critical for the resulted coating structures, which is less significant at high droplet spreading flux. From the given modeling exercises, it has been demonstrated that it is possible using the presented models to better predict the coating qualities, by determining the droplet characteristics during drying at any given process conditions.

Acknowledgements

List of Symbols

A	Droplet area [=] m^2
Cp	Specific heat capacity [=] J/kgK
d_d	Droplet diameter [=] m
h_d	Droplet height [=] m
h	Heat transfer coefficient [=] W/m^{2}K
k	Thermal conductivity (of coating solution) [=] W/mK
m	Droplet mass [=] kg
Q	Heat [=] J
t	Time [=] s
T	Temperature [=] K
U	Velocity [=] m/s
λ	Specific heat of evaporation [=] J/kg
μ	Viscosity [=] Pa.s
θ	Contact angle ($2\tan^{-1}(2h_d/d_d)$) [=]
ρ	Density [=] kg/m^3

Subscript

a	Air
d	Droplet
in	Inlet air
max	Maximum
min	Minimum
o	Initial
p	Core particle
pin	Pinning
s	On core surface
t	In time
wb	Wet bulb

References

1. P. D. Hede, P. Bach, and A. D. Jensen. Small-scale top spray fluidized bed coating: Granule impact strength, agglomeration tendency and coating layer morphology, Powder Technology. 176:156-167 (2007).

2. N. Takei, K. Unosawa, and S. Matsumoto. Effect of the spray-drying process on the properties of coated films in fludized bed granular coaters, Advanced Powder Technology. 13:333-342 (2002).

3. K. Saleh, R. Cherif, and M. Hemati. An experimental study of fluidized-bed coating: influence of operating conditions on growth rate and mechanism, Advanced Powder Technology. 10:255-277 (1999).

4. Y.-S. Wu, L. J. Van Vliet, H. W. Frijlink, and K. Voort Maarschalk.
Pore size distribution in tablets measured with a morphological sieve, International Journal of Pharmaceutics. 342:176-183 (2007).

5. Laksmana, F. L., Koning, A., Hartman Kok, P. J. A., Vromans, H., Frijlink, H. W., and Voort Maarschalk, K. Imaging and quantifying the effects of different process parameters on the quality of particle coating in fluidized bed coater in Proceedings of the 6th World Meeting on Pharmaceutics, Biopharmaceutics and Pharmaceutical Technology (2008).

6. W. E. Ranz and W. R. Marshall. Evaporation from drops, Chemical Engineering and Processing. 48:141-146 (1952).

7. M. Ikegawa and H. Azuma. Droplet behaviors on substrates in thin-film formation using ink-jet printing, JSME Int J Series B. 47:490-496 (2004).

8. S. Saritha and P. Neogi. Wetting kinetics of a thin film evaporating in air, Physics of Fluids. 19:1-6 (2007).

9. M. Kaneda, H. Ishizuka, Y. Sakai, J. Fukai, and S. T. A. Yasutake. Film formation from polymer solution using inkjet printing method, AIChE Journal. 53:1100-1108 (2007).
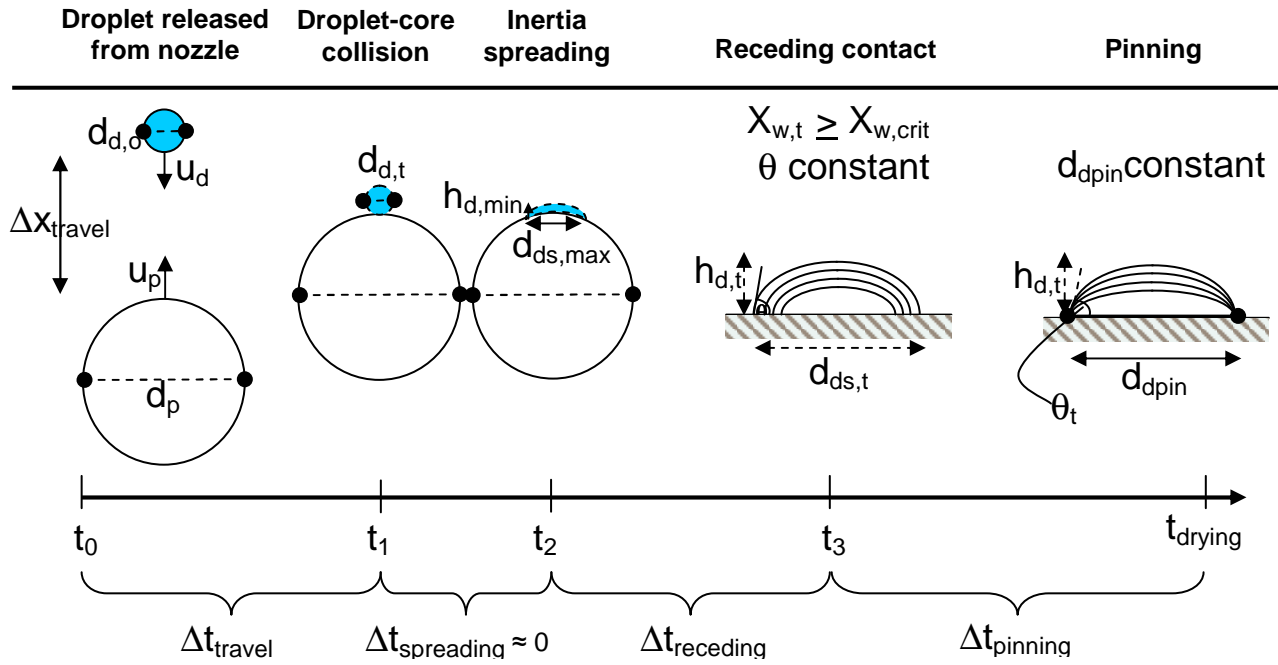
Droplet released from nozzle **Droplet-core collision** **Inertia spreading** **Receding contact** **Pinning**

$d_{d,o}$ u_d

Δx_{travel}

u_p

d_p

$d_{d,t}$ $h_{d,min}$ $d_{ds,max}$

$X_{w,t} \geq X_{w,crit}$
θ constant

$h_{d,t}$ $d_{ds,t}$

d_{dpin} constant

$h_{d,t'}$ θ_t d_{dpin}

t_0 t_1 t_2 t_3 t_{drying}

Δt_{travel} $\Delta t_{spreading} \approx 0$ $\Delta t_{receding}$ $\Delta t_{pinning}$

Figure 1. Schematic description of a droplet's journey inside a fluidized bed coater
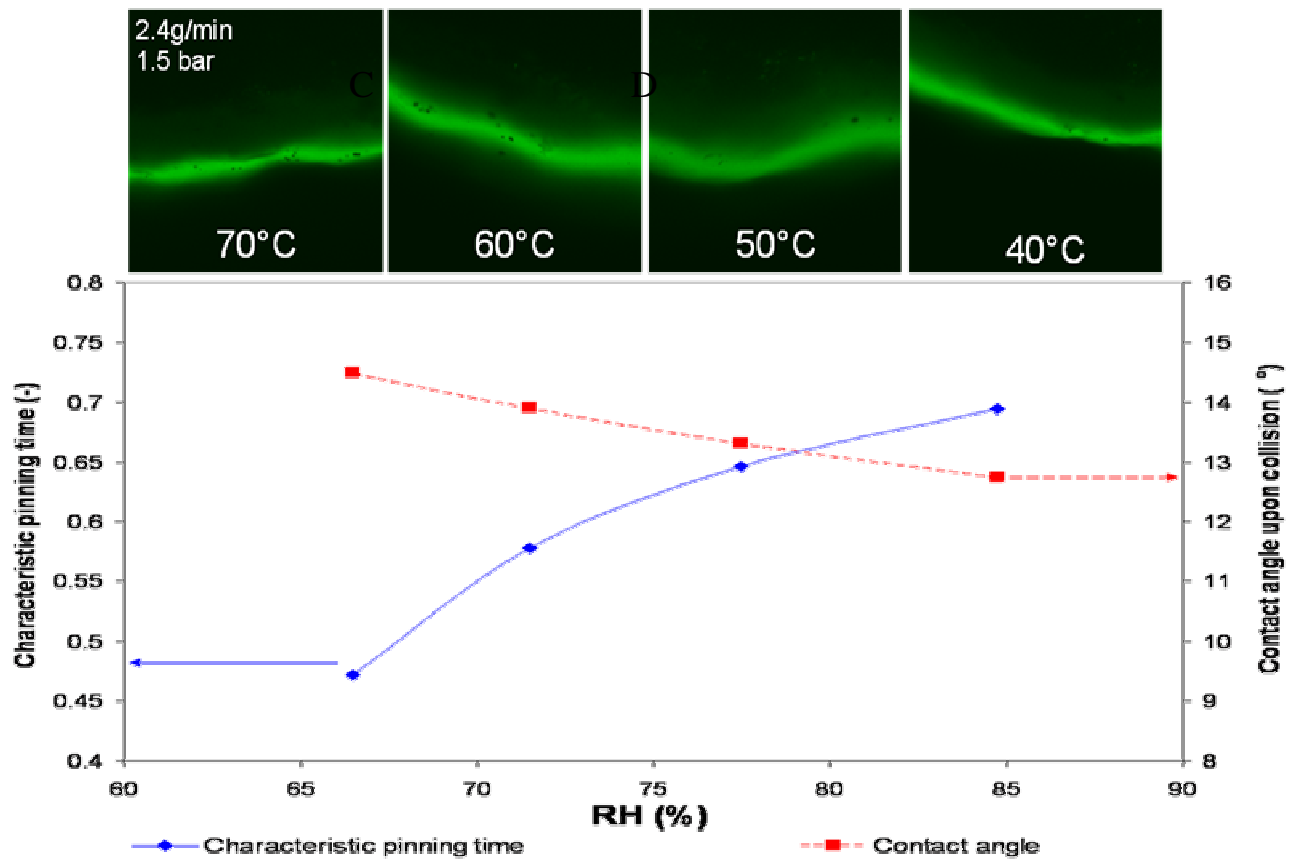
Figure 2. Influence of drying temperature on the characteristic pinning time and contact angle of the droplet upon collision and its impact on the coating structures.
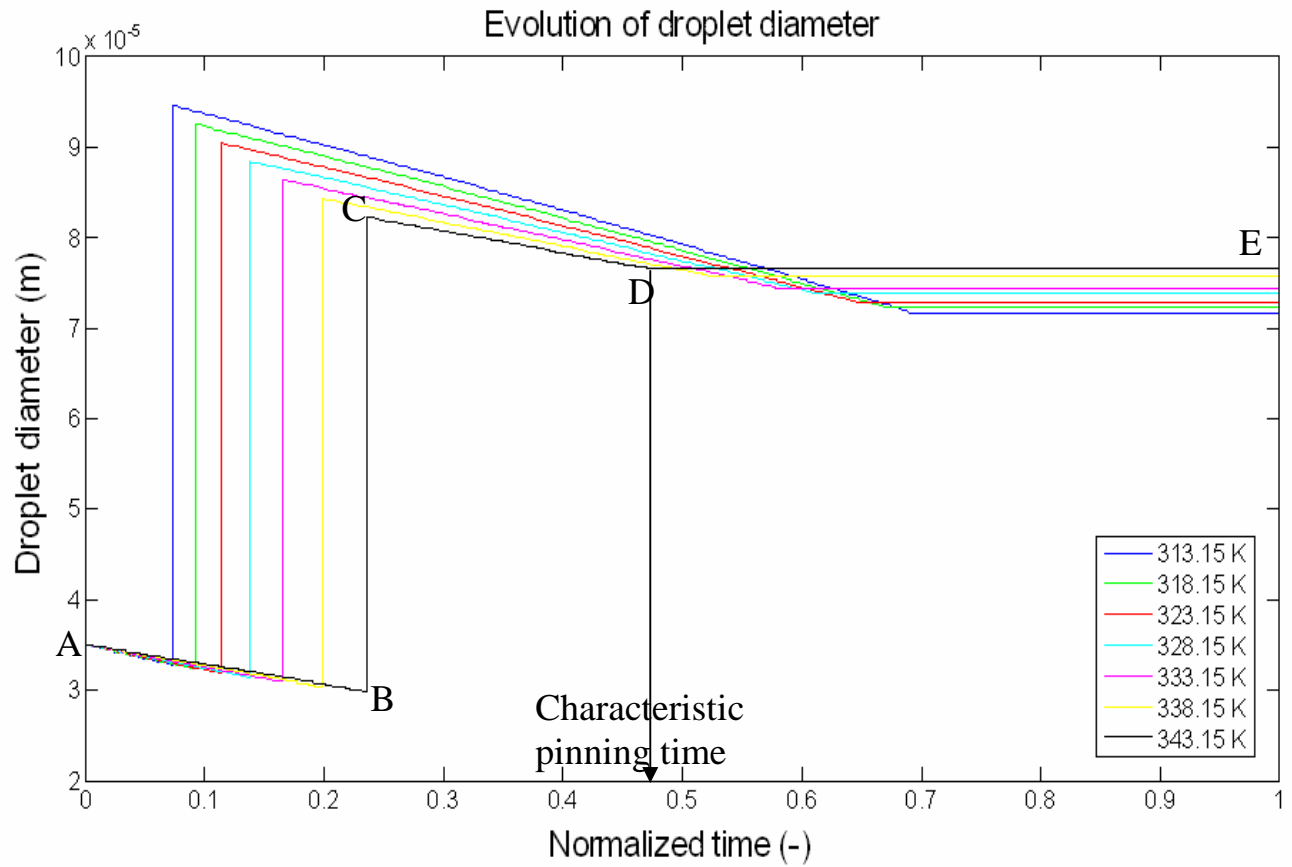
Figure 3. Evolution of droplet diameter during drying in a fluidized bed coater. Point A: Droplet is released from the nozzle; B: Droplet hits a core particle; C: Droplet maximally spreads on a core surface; C-D: Receding contact line evaporation regime, D-E: Pinning evaporation regime.
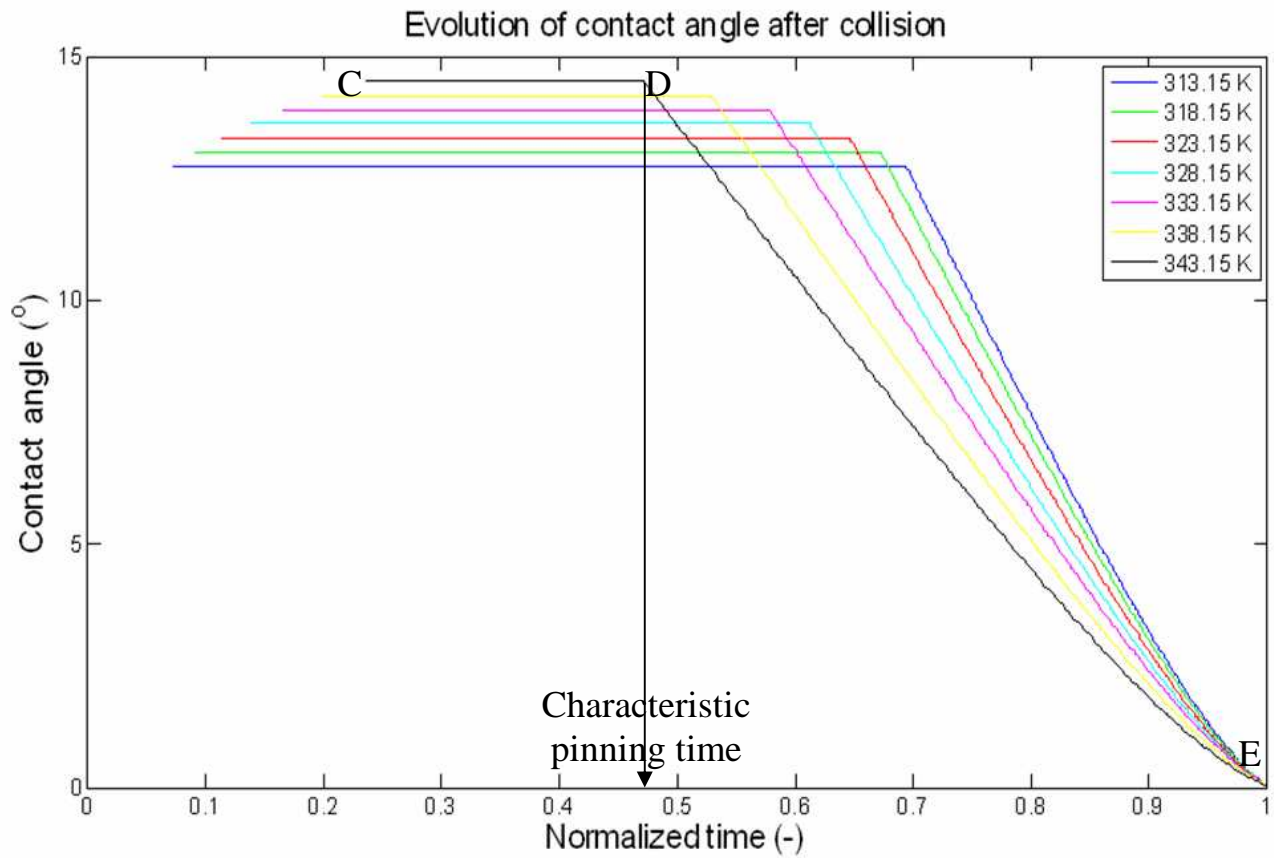
Figure 4. Evolution of droplet shape factor (ratio between droplet height and diameter) during drying in a fluidized bed coater. Point C: Droplet maximally spreads on a core surface; C-D: Receding contact line evaporation regime, D-E: Pinning evaporation regime.
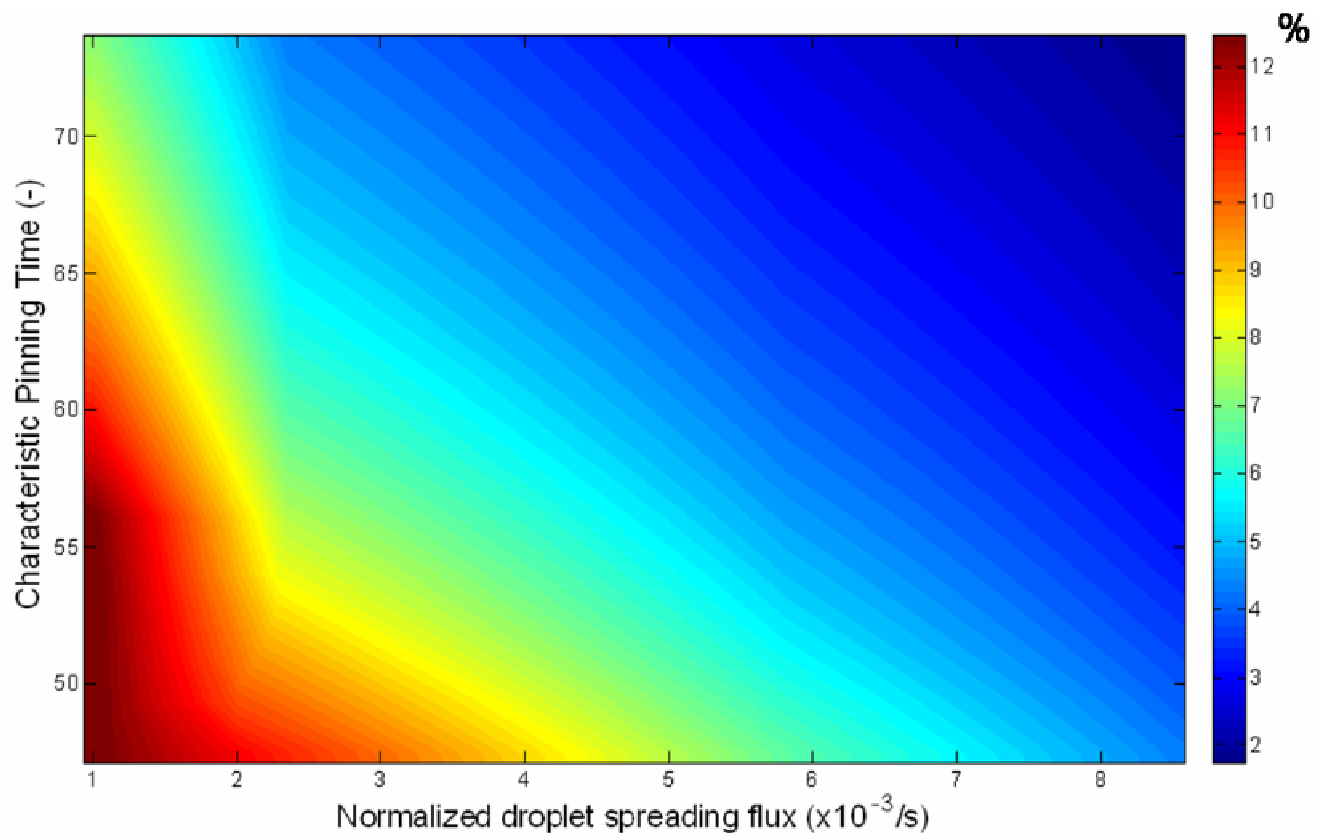
Figure 5. Influence of the characteristic pinning time and normalized droplet spreading flux on the coating porosity.